

## Spreading of Energetic Submerged Fountains Impinging on a Rigid Surface

D. M. Holstein and C. J. Lemckert

School of Engineering  
 Griffith University, Southport, Queensland, 4215, AUSTRALIA

### Abstract

Laboratory experiments and dimensional considerations were used to investigate the spreading behaviour of negatively buoyant axisymmetric vertical fountains after they impinged upon a rigid horizontal surface within an initially homogeneous and quiescent ambient. The distance to which the fountain fluid spread radially along the surface before rising back into the ambient (due to negative buoyancy) was found to be a function of the source radius, the source Froude number and the depth at which the fluid was injected. For example, the greater the source Froude number, and hence initial momentum, the greater the spread of the surface flow for the same injection depth and source radius.

### Introduction

Submerged fountains are created when a light fluid is propelled vertically downwards into a denser miscible ambient (see Figure 1.a.), or when a heavy fluid is injected vertically upward into a lighter ambient. Following release from its source the fountain fluid penetrates to a maximum distance from the source, then stops and falls back onto and/or around the inflow. Ambient fluid is constantly being entrained throughout the flow process, which results in the density difference between the injected fluid and the ambient decreasing with travel time (eg. [1,2,3]).

Fountains occur in many natural and man-made situations. For example, they can be found in parks as display features, in water supply reservoirs (when destratification systems are in operation), and in magma chambers. They can therefore play an important role in transferring mass, momentum and/or energy from one point to another.

Significant studies have been undertaken on fountains (in an effectively infinitely deep ambient) to study the dilution, momentum transfer and the maximum vertical distance the fountain fluid will travel from the source before negative buoyancy forces it to change direction (eg. [1,2,3,4,5]). However, no studies have been cited which examine how far a fountain would spread if the fountain fluid impinged on a surface before reaching its maximum vertical travel distance (see Figure 1.b and 2). This study aimed to address this specific issue as such impinging situations occur in a number of situations [4].

### Scaling Considerations

The fountain source geometry ( $r_o$  for a circular pipe), mean fountain exit velocity ( $u$ ), and initial density difference between the fountain ( $\rho_f$ ) and ambient fluids ( $\rho_2$ ) and the acceleration due to gravity ( $g$ ) are of particular importance in the study of fountains. These variables determine the parameters of volume flux,  $Q$ , momentum flux,  $M$ , and buoyancy flux,  $F$  [1,2,3,4], which are defined as:

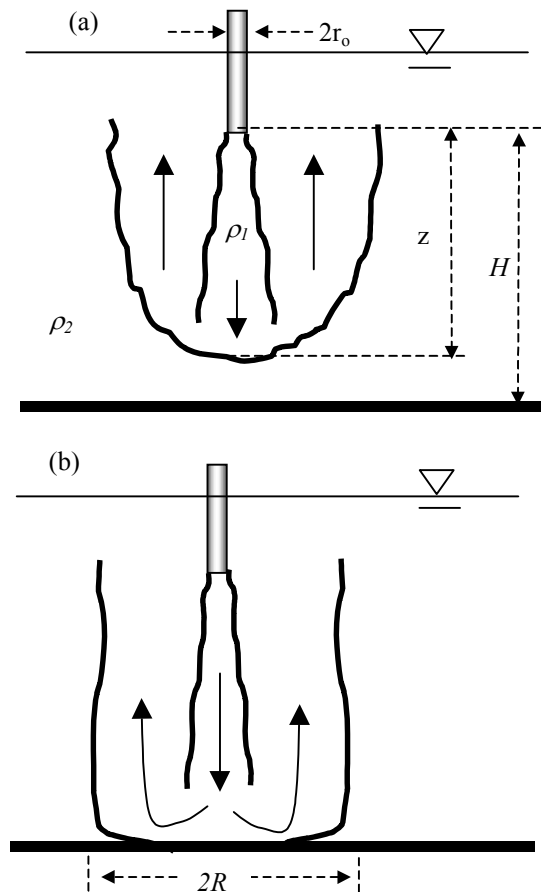


Figure 1. Schematic of a submerged fountain (a) non-impinging and (b) impinging on a flat surface. The solid arrows indicate the major flow directions.

$$\begin{aligned} Q &= \pi r_o^2 u \\ M &= \pi r_o^2 u^2 \\ F &= \pi r_o^2 u \Delta \end{aligned} \quad (1)$$

where  $\Delta = g(\rho_f - \rho_2)/\rho_2$  is the buoyant acceleration. The height of penetration ( $z$ ) a fountain reaches before the direction of the fluid is reversed due to negative buoyancy, is a function of the above parameters:

$$z = f(Q, M, F) \quad (2)$$

After the initial maximum penetration has been reached (following the initiation of a fountain) the height of the fountain decreases to a quasi-steady mean value,  $z_m$ , due to the turbulent interaction between the downflow and upflow. It is at this terminal height that the fluid forms a ring at the outer edge of the

upflow before ascending as a circular line plume in which the fluxes of volume and buoyancy are distributed around a ring [4,5]. The constant mixing of fluid in the fountain (hence dilution) can be estimated using a simple formula (eg. [6]), however, the ‘double’ fountain structure results in a more accurate model being required to relate the dilution to the source conditions.

When  $z_m$  is large in comparison with  $r_o$ , the source is effectively a point and thus  $Q$  can be ignored. Therefore, all the properties of the flow can be scaled in terms of a combination of  $M$  and  $F$ . Dimensional consistency requires that [3]:

$$z_m = CM_o^{3/4} F_o^{-1/2} = r_o C_1 Fr_o = r_o C_1 \frac{w_o}{\sqrt{r_o \Delta_o}} \quad (3)$$

where  $C$  is a constant,  $C_1$  is a constant in the range of 2.46 – 4.18 for point source jets,  $Fr_o$  is the Froude number of the source,  $w_o$  is the top-hat velocity and the subscript  $o$  defined at the source point.

If the distance from the jet source to the opposite boundary of the ambient enclosure,  $H < z_o$ , the fountain will impinge on that surface and spread out radially to a distance,  $R$ , before rising back around the downward flow (Fig 1.b). If the total travel distance of a fluid particle from the source is defined as  $H+R$  then Eq. [3] can be re-written as (after [7]):

$$\frac{H+R}{r_o} = C_2 Fr^n \quad (4)$$

where  $C_2$  and  $n$  are constants to be found experimentally. Kuruppu and Lemckert [7] found that for impinging water jets in air Eq. [4] has the form  $(H+R)/2r_o = 2.1(w_o^2/(2r_o g))^{0.7}$  with a correlation coefficient of 0.92 (NB the equation in [7] was incorrectly printed; the values presented here are the correct ones). The question is: does Eq. [4] also apply for submerged fountains? If it does not, can a better or more correct form be determined?

### Experimental Methodology

The experiments were carried out in an 1800mm square and 800mm deep glass tank filled with a salt water solution. The floor of this tank performed the function of the rigid surface on which the fountains impinged. The fresh water buoyant fountain source originated from a 120 litre insulated reservoir and was pumped into the tank through a 10.9 mm vertical nozzle using a Little Pump Co. model 1-MD pump and a Dataflow compact flowmeter to control and monitor inflow rates. The nozzle was situated away from the sides of the tank and supported by a steel frame (a schematic of the experimental arrangement minus the reservoir and flow controls is depicted in Figure 1.b).

Conductivity and temperature measurements were obtained using a calibrated *in-situ* (Precision Measurement Engineering, USA model 125) micro-scale probe with sensor resolutions of  $1 \times 10^{-3}$  °C and  $2 \times 10^{-5}$  Sm<sup>-1</sup>, spatial resolution of +/-2mm and a time response of approximately 0.02 and 0.004 s respectively. Voltage signals from the probe were recorded through a Labtech Notebook BUILD-TIMEpro software interface. The output voltages from the micro-scale probe provided conductivity and temperature readings at 20hz, and were calibrated daily against an ATI Orion - model 135 conductivity meter.

The microstructure probe was fixed to two Velmex VP9000 series stepping motor controlled sliders that permitted two-

dimensional (vertical and horizontal) traverses across the fountain. The probe was traversed horizontally through the fountain at five equidistant and intermittent vertical heights, with 6x400 mm individual horizontal traverses being performed at each of these vertical heights. The width of the fountains could then be readily determined.

Three lengths of brass pipe were selected to vary the distance of the fountain exit point to the bed. These gave  $H = 75, 133$  and 150mm. Five variations in salt concentration, and hence ambient density, were examined for each injection height. The densities varied from 1001.55 kg/m<sup>3</sup> to 1008.81 kg/m<sup>3</sup> over the range of experiments. Additionally, five injection flow rates for each density were performed with Reynolds numbers ranging from  $440 < Re (= 2w_o r_o / \nu) < 3153$ , where  $\nu$  is viscosity. Both non-impinging and impinging fountains were produced, with the data presented here corresponding only to those experiments where the fountain impinged (see Figure 2).

### Results and Discussion

Two regions of fountain flow were observed in the experiments – the downward flowing core region and the buoyant upward flowing annular plume (see Figures 1 and 2). One feature that is apparent in Figure 2 is that once the jetting fountain fluid hits the plate it spreads horizontally, and that after leaving the plate, due to the effects of negative buoyancy, it continues to spread radially before ascending. This is different from impinging water fountains in air where the spreading fluid appears to stick to the surface before moving back around the jetting fountain fluid [7].

The total plume width ( $2R$ ) was determined from the individual traverses at each transect. As shown in Figures 3 and 4 the position of the outer edge of the annular plume and the boundary between downward and upward flows were readily discernible by a variation in density as the probe traversed through the fountain. The core of the fountain was composed of lower density fluid than that of the buoyant plume, whilst the density of the plume was less than the surrounding ambient. The densities of the core and upflow region increased due to entrainment of denser surrounding fluid; hence the density of the core region was lower having had less time for entrainment.

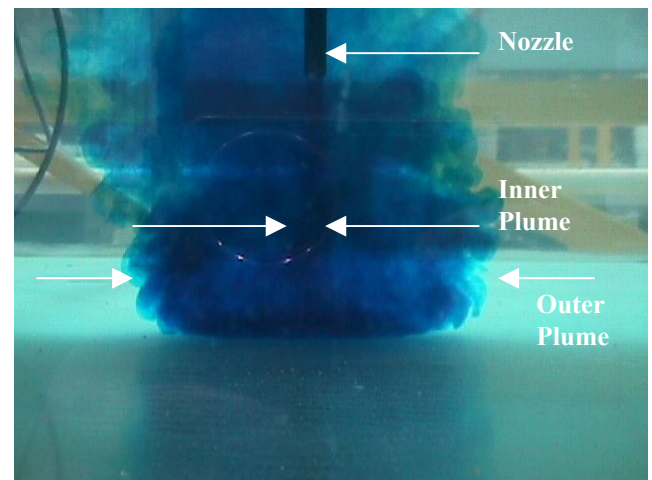


Figure 2. Example of a fountain impinging upon the base of the experimental tank. For clarity, the fountain fluid was dyed blue.

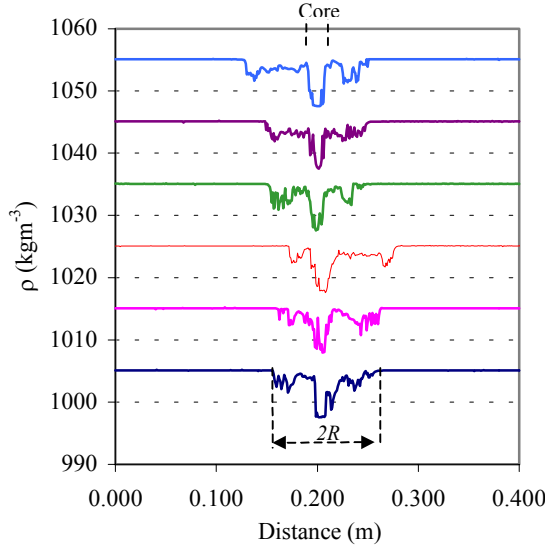


Figure 3. Example density transects derived during one experiment 15 mm above the tank base. For clarity each successive traverse has been displaced by  $10 \text{ kgm}^{-3}$ . In this experiment  $r_o=5.45 \text{ mm}$ ,  $H=75\text{mm}$  and  $Fr_o=8.58$ . The core region and maximum radius are indicated. NB how  $R$  varies from one traverse to another.

The bottom traverse (as shown in Figure 3) was performed 15 mm from the base of the tank, and corresponded to the zone where there was no further horizontal motion resulting from the impinging process. After this distance from the plate, the time-averaged average plume width appeared to remain relatively constant with time and distance. However, as shown in Figure 3, the width did vary from one traverse to another. The variation was found to be significantly greater than the spatial resolution of the conductivity probe. A similar result was found by [3, 6] when fountains did not impinge. Figure 3 also shows how the fountain wanders about its centre line and the variation in densities that can be encountered from one transect to another, even though all the source flow conditions were constant for each successive traverse. This wandering and change in  $R$  from one traverse to another resulted from the unsteady nature of submerged fountains, which consist of a number of large to small eddy structure rather than a continuous steady flow. Since the wandering is three-dimensional and the traversing were only two-dimensional than the recorded profiles may not have passed through the fountain centre line. This may act to give apparently slightly smaller widths and a greater range in estimates of individual plume widths.

Figure 4 shows how averaging the individual traverses from one elevation acts to smooth out the large variations observed in the individual density profiles (Figure 3). This averaging also has the effect of artificially increasing the outer fountain width, as the influence of plume wandering is present. It is for this reason that when fountain widths were evaluated individual transects were examined and a mean width determined from the average of the individual realisations.

Estimates of  $R$  from each transect 15 mm above the plate (as presented in Figure 3) were determined by finding the distance between the outer boundaries of the rising plume as recorded by an individual traverse. These individual estimates were then averaged together to give a mean rising plume radius. For Figure 3 the mean radius was  $0.055\text{m}$  with a standard deviation of

$0.005\text{m}$ , which exceeds the spatial resolution of the conductivity probe. In what follows the use of  $R$  from now on refers to a mean value calculated over 6 traverses.

Analysis of the data revealed that Eq. [4] could be used to model the spreading radius (15 mm above the tank base) as long as  $H$  was kept constant (see Figure 5). For each  $H$   $n$  was found to remain nearly constant. However, the 'constant'  $C_2$  was found to vary from one  $H$  to another, with its value increasing as  $H$  increased (see Table 1).

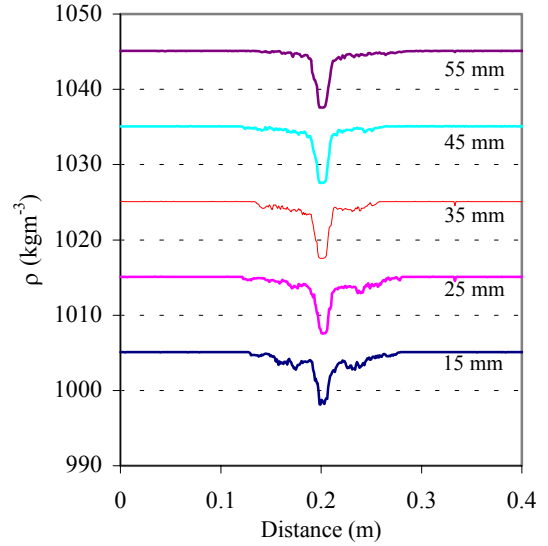


Figure 4. Example density transects derived during one experiment at the 5 elevations above the bed (at 15, 25, 35, 45 and 55 mm). In this figure the 6 individual transects from each elevation have been averaged together. For clarity each successive traverse has been displaced by  $10 \text{ kgm}^{-3}$ . In this experiment  $r_o=5.45 \text{ mm}$ ,  $H=75\text{mm}$  and  $Fr_o=8.58$ .

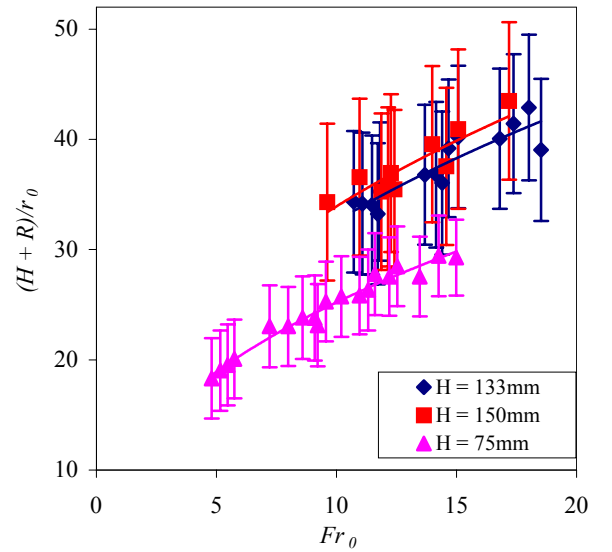


Figure 5. Normalised radius of fountain as a function of  $Fr_o$  for the three injection heights ( $H = 75, 133$  and  $150\text{mm}$ ). The solid lines are those of the lines of best fit to the data (see Table 1). The vertical error bars represent one standard deviation of the derived variable and indicate the relatively large changes that were measured in  $R$ , since  $r_o$  and  $H$  were constant..

Table 1. Results for the application of Eq. [4] to the experimental data for each  $H$ .

$H$ (mm)	Eq. [4] Fit	Correlation Coefficient
75	$(H + R)/r_0 = 9.69Fr_o^{0.42}$	0.975
133	$(H + R)/r_0 = 13.05Fr_o^{0.4}$	0.833
150	$(H + R)/r_0 = 13.54Fr_o^{0.4}$	0.803

The results indicate that Eq. [4] is not quite correct and that a functional form for  $C_2$  must be sought so that all the data can be correctly normalised.

If  $H$  is normalised by the source length scale  $r_o$ , the functional relationship describing  $C_2$  becomes:

$$C_2 = 2.7 \left( \frac{H}{r_0} \right)^{0.5} \quad (5)$$

with a correlation coefficient of 0.996. It is recognised that more work needs to be conducted to validate and/or improve the function of  $C_2$ . Based on Eq. [5], it is now possible to write Eq. [4] as:

$$\frac{H + R}{r_0} = 2.7 \left( \frac{H}{r_0} \right)^{0.5} Fr_o^{0.4} \quad (6)$$

Given that the outer width of the plume has a near constant width once any horizontal momentum has been lost (eg. [2,5] and this study), this equation will be applicable at least until the level of the outlet.

## Conclusions

The properties of negatively buoyant jets impinging on a rigid surface in a quiescent and homogeneous ambient have been investigated using detailed laboratory experiments. As the fountains impinged on the rigid surface, they were observed to spread out laterally before rising as an annular plume around the downward flow.

The spreading radius of the fluid as it impinged on the rigid surface was found to be a function of the source Froude number, the source radius and the distance from the fountain source to the impinged surface. The data were well correlated at each individual injection height, and comparable power constants were obtained for each of the three injection heights investigated. A correction factor was introduced to relate the constants obtained from the experiment with the normalised injection height of the source.

## Acknowledgments

The authors would like to thank Charles Allport for assisting with setting up the experimental facility and for the School of Engineering, Griffith University for purchasing various items of equipment used in this study.

## References

- [1] Morton, B. R., (1959), *Forced Plumes*, J. Fluid Mech., 5, 151-163.
- [2] Mizushima, T., Ogino, F., Takeuchi, H. and Ikawa, H., (1982), *An experimental study of vertical turbulent jet with negative buoyancy*, Wärme-und Stoffübertragung, 16, 15-21.

- [3] Turner, J.S. (1966), *Jets and plumes with negative or reversing buoyancy*, J. Fluid Mech., 26 (4), 779-792.
- [4] Baines, W. D., Turner, J.S. and Campbell, I.H., (1989), *Turbulent fountains in an open chamber*, J. Fluid Mech., 212, 557-592.
- [5] Bloomfield, L. J. and Kerr, R. C., (2000), *A theoretical model of a turbulent fountain*, J. Fluid Mech., 424, 197-216.
- [6] Fischer, H. B., List, E. J., Koh, R. C. Y., Imberger, J. & Brooks, N.H., *Mixing in inland and coastal waters*, Academic, 1979.
- [7] Kuruppu, K. and Lemckert, C. J. (2000) *Plunging Radius of Water Fountains Following Impact on a Rigid Surface*, 7th Australasian Heat and Mass Transfer Conference, Townsville, Queensland, Australia, July, 2000, 195-200